



Open Archive Toulouse Archive Ouverte (OATAO)

OATAO is an open access repository that collects the work of Toulouse researchers and makes it freely available over the web where possible.

This is an author-deposited version published in: <http://oatao.univ-toulouse.fr/>
Eprints ID: 5571

To link to this article: DOI: 10.1016/j.carbpol.2011.01.040
URL: <http://dx.doi.org/10.1016/j.carbpol.2011.01.040>

To cite this version:

Robitzer, M. and Tourette, A. and Horga, R. and Valentin, R. and Boissière, M. and Devoisselle, J. M. and Di Renzo, F. and Quignard, F. *Nitrogen sorption as a tool for the characterisation of polysaccharide aerogels.* (2011) Carbohydrate Polymers, vol. 85 (n° 1). pp. 44-53. ISSN 0144-8617

Any correspondence concerning this service should be sent to the repository administrator: staff-oatao@listes.diff.inp-toulouse.fr

Nitrogen sorption as a tool for the characterisation of polysaccharide aerogels

M. Robitzer, A. Tourrette¹, R. Horga, R. Valentin², M. Boissière³, J.M. Devoisselle, F. Di Renzo*, F. Quignard

Institut Charles Gerhardt Montpellier, UMR 5253 CNRS-UM2-ENSCM-UM1, Matériaux Avancés pour la Catalyse et la Santé, ENSCM, 8 rue Ecole Normale, 34296 Montpellier Cedex 5, France

Keywords:

Aerogel
Supercritical drying
Comparison plots
Surface polarity
Adsorption enthalpy
Physisorption
Polysaccharides
Alginate
Chitosan
Chitin
Agar
Carrageenan

A B S T R A C T

Supercritically dried aerogels of several polysaccharides (chitin, chitosan, alginate, alginic acid, κ -carrageenan, and agar) have been characterised by physisorption of N₂. Surface areas as high as 570 m² g⁻¹ have been measured. The nature of the functional groups of the polysaccharide significantly influences the adsorption of N₂ on the surface of the aerogel. The net enthalpy of adsorption increases with the polarity of the surface groups of the polymer, in the order chitin < agar \leq chitosan < carrageenan < alginic acid \sim alginate. The surface area and the mesopore distribution of the aerogels depend both on the dispersion of the parent hydrogel and on the behaviour of each polymer in the drying treatment. Aerogels which retain the dispersion of the parent hydrogel are mainly macroporous (pores larger than 50 nm) while materials liable to shrink upon solvent exchange form mesoporous structures.

1. Introduction

The surface properties of biological materials are at the basis of phenomena like cell adhesion, formation of bacterial films, and recognition between biological units. Surface polarity is a major parameter in controlling the adhesion of cells and bacteria (Absolom et al., 1983; Li & Logan, 2004; van Loosdrecht, Lyklema, Norde, & Zehnder, 1989), a relevant phenomenon in fields as different as safety of surgical devices, colonisation of biomaterials (Elbert & Hubbell, 1996; Tirrell, Kokkoli, & Biesalski, 2002), sensitivity of biological sensors (Chu, Hsu, Soma, & Lo, 2009; Disney, Zheng, Swager, & Seeberger, 2004), membrane fouling (Miura, Watanabe, & Okabe, 2007), and effectiveness of water and sewage treat-

ments (Dhoot & Wheatley, 2003; Liu, Yang, & Li, 2007; Simoni, Bosma, Harms, & Zehnder, 2000; Tufenkji, Dixon, Considine, & Drummond, 2006). Biological recognition phenomena previously only attributed to molecular lock-and-key interactions have been acknowledged to be largely dependent on the adhesion of extended structures (Cherstvy, Kolomeisky, & Kornyshev, 2008; Leckband, 2001; Mammen, Choi, & Whitesides, 1998). Polysaccharides represent an important component of bacterial capsules and they play an important role in cell adhesion (Aronson et al., 1979; Lee et al., 2006; Sadamoto et al., 2004; Schengrund, 2003; Sharon & Ofek, 2000; Sugita-Konishi et al., 2002). Extracellular polysaccharides usually present complex structures and are seldom available in amounts large enough to allow physical characterisation by macroscopic tools. Model systems available in large amount in high surface area formulations can represent a useful model to study the surface energetics of complex polysaccharides. Aerogel formulations of gelling polysaccharides could allow the characterisation of surface polarities by physisorption methods largely used in materials chemistry.

Gelling polysaccharides are natural polyelectrolytes with a high concentration of hydrophilic functional groups (Dumitriu, 1998; Stephen, Phillips, & Williams, 2006). For instance, chitosan, the deacetylated form of chitin, the second most diffused natural

* Corresponding author. Tel.: +33 607508148; fax: +33 467163470.

E-mail address: direnzo@enscm.fr (F. Di Renzo).

¹ Present address: CIRIMAT-ENSIACET, 4 allée Emile Monso, BP 44362, 31342 Toulouse, France.

² Present address: Laboratoire Chimie Agro-Industrielle, UMR 1010 CNRS-INRA-ENSIACET, Université de Toulouse, 118 Route de Narbonne, 31077 Toulouse Cedex 4, France.

³ Present address: Laboratoire Physicochimie des Polymères et des Interfaces, Université de Cergy-Pontoise, 5 mail Gay-Lussac, 95031 Neuville-sur-Oise, France.

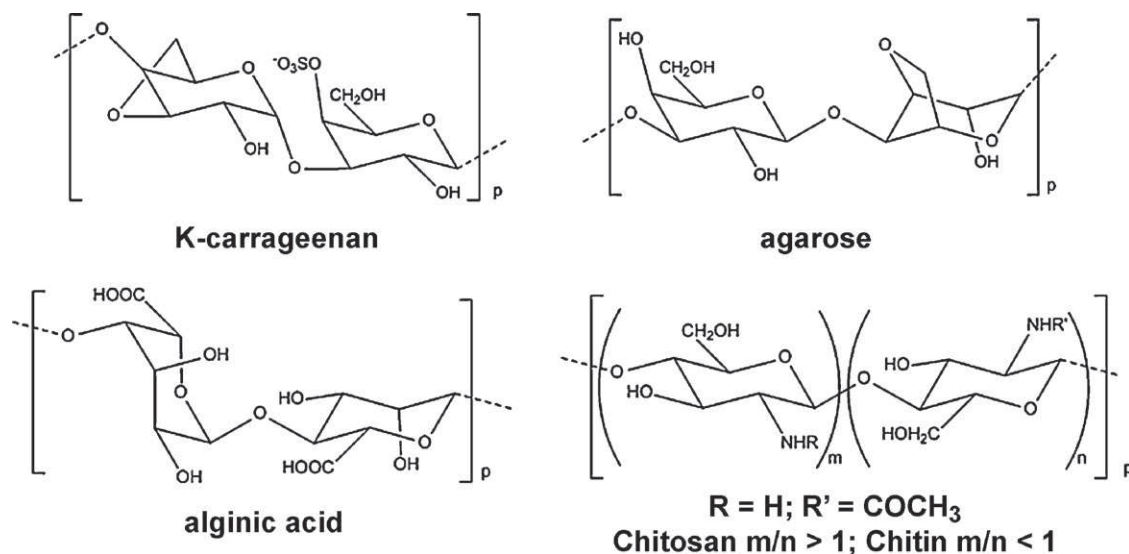


Fig. 1. Repeating modules of gelling polysaccharides.

polysaccharide after cellulose, presents up to 5.8 mmol amino groups per gram of polymer (Roberts, 1992); alginic acid, a polysaccharide extracted from brown seaweeds, presents up to 5.6 mmol carboxylic groups per gram of polymer; κ -carrageenan, another seaweed-extracted polysaccharide, presents up to 2.8 mmol sulphate groups per gram of polymer (see Fig. 1 for a representation of some monomers). In usual hydrogel formulations, most functional groups interact with an aqueous solution. Polysaccharide hydrogels are able to store up to one hundred times their weight of water, trapped in a network of hydrophilic fibrils. This property accounts for their natural occurrence as water reservoirs in plants (Percival & McDowell, 1967; Walter, 1998) and their application as thickening agents in the food industry (Pilnik & Rombouts, 1985) and drug carriers or tissue healing agents in the pharmaceutical and personal care industries (Dhoot & Wheatley, 2003; Drury & Mooney, 2003; Peppas, Hilt, Khademhosseini, & Langer, 2006; Ravi Kumar, Muzzarelli, Sashiwa, & Domb, 2004).

The dispersion of the polysaccharides in the hydrogel is at the basis of their application as supports for enzymatic catalysis in aqueous phase (Dumitriu & Chornet, 1998; Liu, Becker, & Neufeld, 2005). The accessibility of their functional groups renders them effective ion exchangers and complexing agents for remediation (Chassary, Vincent, & Guibal, 2004; Jaafari, Elmaleh, Coma, & Benkhouja, 2001; Laus, Geremias, Vasconcelos, Laranjeira, & Fávère, 2007). The application of these materials as heterogeneous catalysts in the gas phase has been hampered by the shrinkage of the hydrogels during drying (Guibal, 2005; Guibal, Vincent, & Peirano-Blondet, 2007; Vincent & Guibal, 2004). In evaporative drying processes, the tension of the meniscus at the solvent–vapour interface draws together the colloidal units of the gel and brings to the formation of xerogels with minimal surface area (Di Renzo et al., 2005; Valentin, Bonelli, Garrone, Di Renzo, & Quignard, 2007).

Alternative drying methods have been tested to retain in the dry state the dispersion of the parent hydrocolloids. Cryogels obtained by freeze-drying retain the volume of the parent hydrogel but the fine structure of samples thicker than a few micrometers is disrupted by the growth of ice crystals inside the material (Casson & Emery, 1987; Hills et al., 2000). Fast-freezing and pressure-freezing have allowed to extend the field of application of cryopreservation to samples of thickness up to one hundred microns but significant structural damages have been observed for larger specimens (Serp, Mueller, von Stockar, & Marison, 2002a). Drying by evaporation of solvents with low surface tension has allowed to retain

most of the dispersion of polysaccharide gels (White, Budarin, & Clark, 2008). The best structure preservation results have been obtained by CO₂ supercritical drying, a technique currently used to preserve the fine structure of gels as different as silica-based adsorbents, insulation materials, optical fibers, polymer membranes or carbon precursors (Cardea et al., 2009; Pekala, 1989; Pierre & Pajonk, 2002). Supercritically dried polysaccharide aerogels can present porosities as high as 98% (Partap, Rehman, Jones, & Darr, 2006; Quignard, Valentin, & Di Renzo, 2008; Valentin et al., 2006). The formation of aerogels has allowed to characterise the textural properties of the polysaccharide gels by classical physisorption techniques (Valentin, Molvinger, Quignard, & Di Renzo, 2005; Valentin, Molvinger, Viton, Domard, & Quignard, 2005). Surface areas as high as 570 m² g⁻¹ in the case of alginate and 845 m² g⁻¹ in the case of cross-linked chitosan have been reported (Chang, Chen, & Jiao, 2008; Quignard et al., 2008). Such values of surface area correspond to a significant dispersion of the materials. In the case of a Ca-alginate aerogel, a surface area of 570 m² g⁻¹ corresponds to isolated fibrils of average diameter 4 nm, as calculated further in this article.

The surface properties of polysaccharide aerogels have been a quite neglected research subject, despite their obvious interest for heterogeneous catalysis and as models of biological systems. The IR monitoring of the chemisorption of probe molecules like ammonia or deuterated water (Valentin et al., 2006, 2007) has shown that small reactive molecules penetrate to a significant extent inside the polysaccharide fibrils and react with most functional groups of the polymer. The adsorption of less reactive molecules at lower temperature can bring a different kind of information. The purpose of this contribution is to study the aerogels of several polysaccharides by classical volumetric techniques in order to find information about their morphology and the energetics of physisorption at their surface.

2. Experimental

2.1. Preparation of the samples

2.1.1. Agar beads

A 2% (w/w) agar solution (agarose-D5 Hispanagar) was rapidly heated at the boiling point in a microwave oven. The polymer solution was transferred to a syringe thermostated at 50 °C and added dropwise to a cooled water bath.

2.1.2. Alginate beads

Several Na-alginate with different guluronic content were used and defined as G-X, where X is the percent of guluronic groups: G-20 Protanal FMC Biopolymer, G-35 Sigma-Aldrich, G-45 Cicalgum S500 Sanofi, and G-76 Satialgine SG 800 Systems Bio-Industries. Sodium alginate was dissolved in distilled water at a concentration of 2% (w/w). The polymer solution was added dropwise at room temperature to a stirred MCl_2 (Aldrich, M being Ca^{2+} , Ba^{2+} , Co^{2+} or Cu^{2+}) solution (0.24 mol L^{-1}) or a HCl solution (1 mol L^{-1}) using a syringe with a 0.8 mm diameter needle. The microspheres were cured in the gelation solution for 15 h.

2.1.3. Carrageenan beads

A 2.5% (w/w) κ -carrageenan stock solution was prepared by dispersing κ -carrageenan (*eucheuma cottonii* Sigma 90%) in ultrapure water at 80°C for 30 min. The 2.5% stock solution of κ -carrageenan thermostated at 80°C was dropped into a 0.6 M KCl solution at 5°C under stirring using a syringe with a 0.8 mm diameter needle. The gel beads were aged for 12 h in this solution at 5°C without stirring and hence washed with cold water (Sipahigil & Dortunc, 2001).

2.1.4. Squid-pen chitosan beads

An aqueous solution of chitosan from β -chitin (Mahtani Chitosan PVT, degree of acetylation lower than 5%, as measured by NMR spectroscopy, weight-average molecular weight $M_w = 200\,000 \text{ g mol}^{-1}$, measured by light scattering) was obtained by dissolving 1 g of chitosan in 100 mL of a solution of acetic acid 0.055 mol L^{-1} . This solution was dropped into a NaOH solution (4 mol L^{-1}) through a 0.8 mm syringe needle. The beads of chitosan from β -chitin, shorthanded here as β -chitosan, were stored in the alkaline solution for 2 h, and then filtered and washed with water.

2.1.5. Crab-shell chitosan beads

A 2.5% aqueous solution of purified chitosan from α -chitin (Aldrich, degree of acetylation of 10% as measured by IR spectroscopy, $M_w = 700\,000 \text{ g mol}^{-1}$ determined by viscosimetry) was formed by stirring 2 h at room temperature using with the stoichiometric amount of acetic acid with respect to the amount of NH_2 functions. Gelation was obtained by dropping the chitosan solution into a 4 mol L^{-1} NaOH solution through a 0.8 mm gauge syringe needle. The beads of chitosan from α -chitin were left in the alkaline solution for 2 h, filtered and washed with demineralised water.

2.1.6. Chitin gel

β -Chitin was obtained by complete reacylation of squid-pen chitosan according to a published procedure (Vachoud, Zydowicz, & Domard, 1997). An aqueous acetic acid (0.5%, w/w) solution of chitosan (1%, w/w) (100 g) was mixed with ethanol (50 mL) and the mixture was left to stand overnight for degassing without stirring. A freshly prepared acetylating solution (6.85 mL ethanol, 0.65 mL acetic anhydride) was slowly added to 20 g of the aqueous alcoholic chitosan solution. The mixture was then stirred for 30 s and transferred to a cylindrical mould. The gel was aged 4 h, and washed twice with ethanol.

2.2. Supercritical drying

To obtain aerogels, the hydrogels were dehydrated by immersion in a series of successive ethanol-water baths of increasing alcohol concentration (10, 30, 50, 70, 90, and 100%) for 15 min each (Martinsen, Storrrø, & Skjåk-Bræk, 1992). Finally, ethanol was replaced by liquid CO_2 and the microspheres were dried under supercritical CO_2 conditions (74 bars, 31.5°C) in a Polaron 3100

apparatus. In the case of chitin, the ethanol-washed gel was directly dried under supercritical CO_2 conditions.

2.3. Volumetric experiments

Adsorption-desorption isotherms of nitrogen at 77 K and argon at 77 and 89 K were registered on a Micromeritics Asap 2010 volumetric apparatus by admitting doses of N_2 in a measurement cell. The aerogel samples were previously outgassed in situ at 323 K until a 0.4 Pa stable static vacuum was reached. Surface area and energetical parameter $C(\text{BET})$ were evaluated by the BET method (Rouquerol, Rouquerol, & Sing, 1999). The net molar energy of adsorption $\Delta E = E_{\text{ads}} - E_L$, where E_{ads} is the molar adsorption energy of N_2 on the surface and E_L is the liquefaction energy of bulk N_2 (5.6 kJ mol^{-1}), was calculated as $\Delta E = RT \ln C(\text{BET})$. A molecular area 0.162 nm^2 for an adsorbed molecule of N_2 was assumed in the calculation of the surface area.

The surface area can provide information on the average diameter D of the fibrils, assumed as cylindrical, by the formula $D = 4000 A^{-1} \rho^{-1}$, where D is the diameter in nm, A the surface area in $\text{m}^2 \text{ g}^{-1}$, and ρ the volumic mass in g cm^{-3} . In the case of polysaccharides, this evaluation is a crude approximation due to difficulties in determining the correct bulk density of the fibrils. Most literature values deal with the density of crystallized polymers, likely slightly higher than the bulk density of the fibril material. These literature values can be accepted as a first approximation and are 1.15 g cm^{-3} for agar (Foord & Atkins, 1989), 1.48 for κ -carrageenan (Millane, Chandrasekaran, Arnott, & Dea, 1988), 1.42 for β -chitin (Neville, Parry, & Woodhead-Galloway, 1976), and 1.67 for chitosan (Okuyama, Noguchi, Miyazawa, Yui, & Ogawa, 1997). In the case of alginate, the literature density of crystalline guluronic acid (1.62 g cm^{-3}) and Calciumuronate (1.79 g cm^{-3}) (Atkins, Nieduszyński, Mackie, Parker, & Smolko, 1973; Mackie, Perez, Rizzo, Taravel, & Vignon, 1983) have been used, as guluronate is the only type of block copolymer of ionotropic alginate for which crystallographic data are available.

The agreement with the layer-by-layer mechanism of adsorption was evaluated by the α_S method (Gregg & Sing, 1982). A composite reference silica isotherm was used, based on adsorption data for fumed silica Aerosil 200 for $\alpha_S < 0.30$ and LiChrospher Si-1000 precipitated silica (Jaroniec, Kruk, & Olivier, 1999) for higher values. Mesopore size was evaluated from the desorption branch of the isotherm by the DFT method, proved more reliable than the widely used BJH method (Galarneau, Desplandier, Dutartre, & Di Renzo, 1999; Neimark & Ravikovitch, 2001). The cylindrical model of mesopore geometry is used for sake of comparison, due to the lack of suitable models to describe the correlation between capillary condensation pressure and geometry in an open network of rods. The total porosity, including macroporosity and mesoporosity, was evaluated from the volume/mass ratio of the aerogel.

3. Results

3.1. Texture of the aerogels

The N_2 adsorption isotherms for some typical polysaccharide aerogels are reported in Fig. 2. The low-pressure adsorption step allows to evaluate the volume of an adsorbed monolayer, from which the surface area of the sample is calculated. The surface areas for several typical polysaccharide aerogels are reported in Table 1.

N_2 physisorption isotherms provide information on the area of the surface but do not provide unequivocal information on the

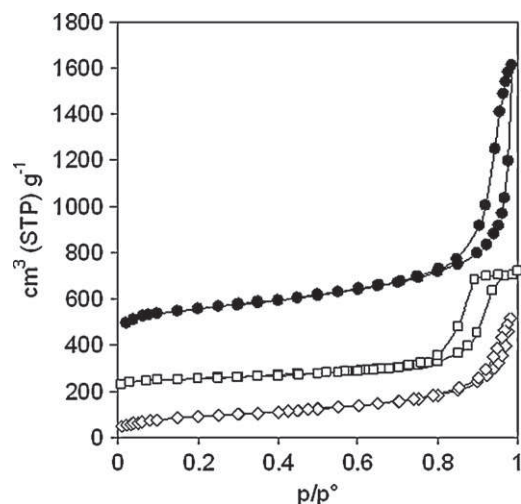


Fig. 2. N₂ adsorption isotherms at 77 K on aerogels of (filled circles) Ca-alginate, (void lozenges) agar and (void squares) κ -carrageenan. Isotherms are shifted by 200 cm³ g⁻¹.

shape of the surface. A better understanding of the texture of the solids can be obtained by coupling physisorption data with other techniques of characterisation, like scanning electron microscopy. A micrograph of the cross-section of a typical Ca-alginate aerogel is reported in Fig. 3a and shows an open framework of isolated fibrils with a diameter 5–8 nm and an average length near 200 nm. Bundles of three or four fibrils are a rare occurrence. The most frequent contact between fibrils is at nodes connecting the ends of three fibrils. This kind of branching suggests that the fibrils have been formed as a network and the aerogel is not the result of the random aggregation of independently formed fibrils. A texture characterised by an open network of fibrils is representative

of most freeze-dried or supercritically dried gels of polysaccharides and other semi-crystalline polymers (Daniel et al., 2005; Kanzawa, Koreeda, Harada, & Harada, 1989; Kanzawa, Koreeda, Harada, Okuyama, & Harada, 1990; Quignard et al., 2008; Serp, et al., 2002a; Serp, Mueller, von Stockar, & Marison, 2002b; Valentin, Molvinger, Quignard, & Di Renzo, 2005). This kind of texture is also well known in biological media, for instance for polysaccharide capsules around yeasts and bacteria (Bayer, 1990; Kopecká, Phaff, & Fleet, 1974).

The fibrillar texture of the solid justifies the use of a simplified cylindrical model to evaluate the size of the fibrils from the surface area measured by N₂ adsorption. The calculated diameters for cylindrical rods with a surface area equivalent to the polysaccharide micelles are reported in Table 1 and vary from 3 to 4 nm for the aerogels of the highest surface area to 16 nm for the aerogel with the lowest surface area. This domain of fibril size is in good agreement with the results of other techniques, like AFM of supported gels (Decho, 1999; Maurstad, Danielsen, & Stokke, 2003; Sletmoen, Maurstad, Sikorski, Smestad Paulsen, & Stokke, 2003) or SAXS (Robitzer, David, Rochas, Di Renzo, & Quignard, 2008).

The shape of the N₂ physisorption isotherms provides information on the porosity of the system, albeit not all porosity can be detected by this technique. For instance, most cavities of the network of fibrils of Fig. 3a are larger than 100 nm. Such cavities are too wide to be detected by N₂ adsorption methods, which are limited to the analysis of mesopores, viz. pores with size between 2 and 50 nm (Sing et al., 1985). The porosity data reported in Table 1 confirm that mesoporosity is only a small fraction of the total porosity of the aerogel (excepted for carrageenan). For most aerogels, mesopores are representative of the relatively unfrequent zones of contact between fibrils.

Mesopore size distributions for several polysaccharide aerogels are reported in Fig. 4. Mesopore size is quite characteristic for the aerogels of each type of polysaccharide and can be correlated to parts of the solid in which the distance between secondary units is

Table 1
Typical textural data for polysaccharide aerogels.

Aerogel	Surface area (m ² g ⁻¹)	Fibril diameter (nm)	Average mesopore size (nm)	Mesopore volume (cm ³ g ⁻¹)	Total porosity (cm ³ g ⁻¹)	% Volume shrinkage upon drying
κ -Carrageenan	200	11	18	0.96	1	95
Agar	320	11	36	0.23	7	92
Chitosan from α -chitin	330	7	12	0.57	15	60
Chitosan from β -chitin	150	16	25	0.18	19	51
β -Chitin	560	5	20	1.24	16	76 ^a
Alginic acid	390	6	20	0.89	38	22
Ca-alginate	570	4	37	1.16	39	20

^a Drying shrinkage measured from the alcohol-exchanged form.

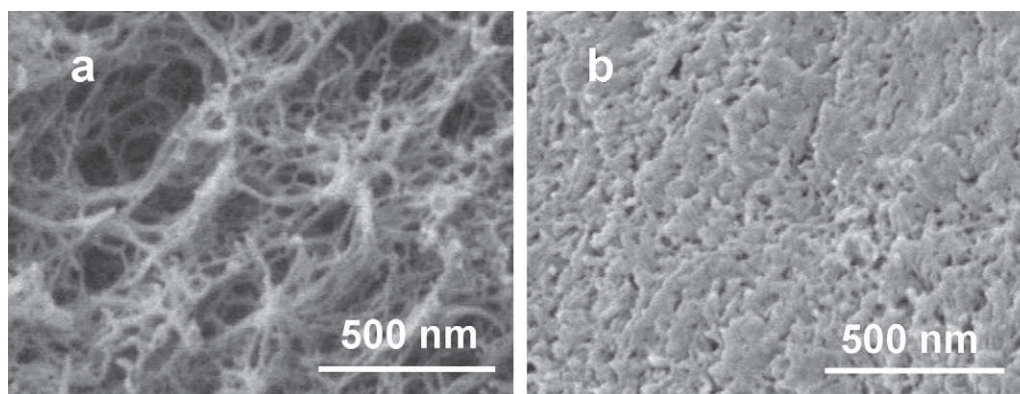


Fig. 3. Scanning electron micrographs of cross-sections of (a) Ca-alginate and (b) κ -carrageenan aerogels.

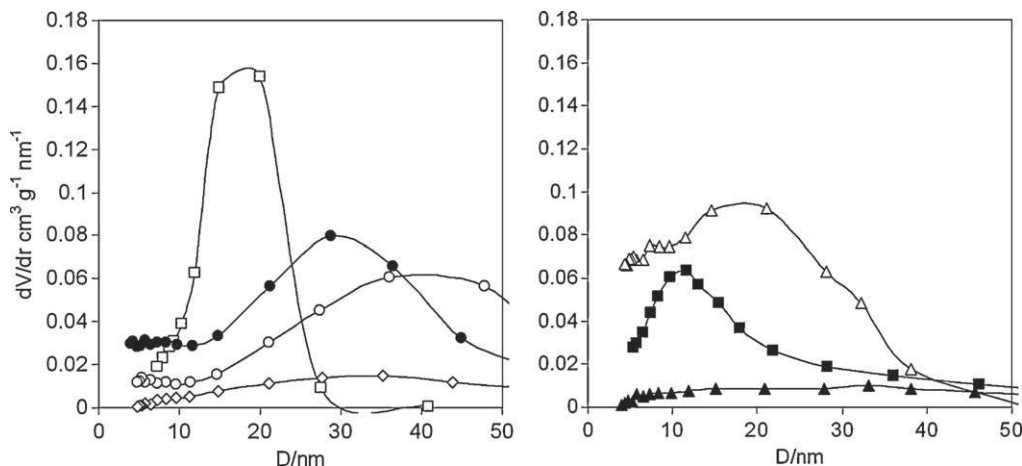


Fig. 4. Pore size distributions for aerogels of κ -carrageenan (void squares), Ca-alginate (filled circles), alginic acid (void circles), agar (void lozenges), β -chitin (void triangles), chitosan from α -chitin (filled squares) and chitosan from β -chitin (filled triangles).

smaller than about 50 nm. The scanning electron micrograph of an alginate gel reported in Fig. 3a shows area of different density in the distribution of the fibrils. This heterogeneity is reflected in the mesopore size distribution of the aerogels of alginate or alginic acid reported in Fig. 4. Such very broad mesopore size distributions, with no solution of continuity with the domain of macropores (pores larger than 50 nm) are clearly related to heterogeneities in the gel density.

A very different pattern is followed by κ -carrageenan, a rare instance of polysaccharide gel which undergoes severe shrinkage upon the supercritical drying procedure (Boissière, Tourrette, Devoisselle, Di Renzo, & Quignard, 2006). A micrograph of the cross-section of this collapsed gel is shown in Fig. 3b. The solid has a much more compact aspect than the alginate aerogel of Fig. 3a. A residual shrunk fibrillar structure is still present, with visible cavities between 10 and 30 nm. The porosity data reported in Tab. 1 indicate that mesoporosity represents the total porosity. The distribution of pore size shown in Fig. 4 is quite narrow and centred around 18 nm, indicating that the shrinkage of the gel has formed a uniformly tight network of secondary units.

Another pattern of porosity is observed for agar aerogels, in which a negligible amount of mesoporosity is observed. This suggests that, despite the significant shrinkage underwent by the gel in the drying process, the secondary units of the polymer are uniformly separated at distances higher than the upper limit detectable by nitrogen adsorption. A similar pattern is also observed in the aerogels of chitosan formed by deacetylation of β -chitin. It is interesting to observe that the origin of the chitosan significantly affects the physisorption pattern of the aerogel. Chitosan formed by deacetylation of α -chitin presents a quite narrow distribution of mesopore size and a mesopore volume which represents only a small fraction of the total porosity. It is tempting to correlate the adsorption pattern of the aerogels to the properties of the parent gels. Polymer threads of partially deacetylated chitosan from β -chitin are well isolated in solution, while chitosan from α -chitin presents both isolated chains and more organized parts which retain some structure of the parent α -chitin (Lamarque, Viton, & Domard, 2004). It is possible to correlate the non-mesoporous part of the chitosan aerogels with a uniform gel formed from the isolated polymer chains presents in both kinds of chitosan, whereas the mesoporous parts of the aerogel of chitosan from α -chitin could correspond to cavities related to a residual chitin-like organisation. Indeed, chitin aerogel presents a significant mesoporosity well-separated from macroporosity, with a quite broad distribution of mesopore size.

3.2. Surface properties of the polymers

Comparison plots are widely used to identify the adsorption mechanisms, especially to differentiate layer-by-layer adsorption on a surface from condensation in micropores or mesopores (Lippens & de Boer, 1965). In a comparison plot, the amount adsorbed on the sample at a given pressure is plotted against the amount adsorbed at the same pressure on a reference non-porous adsorbent. In such a graph, a linear correlation between the amount adsorbed on the sample under investigation and the reference adsorbent indicates that the adsorption takes place by the same mechanism on the two surfaces. The slope of the plot corresponds to the ratio between the surface areas of the two adsorbents. The α_s plot is a comparison plot in which the abscissa are normalised on the amount adsorbed on the reference isotherm at $p/p^0 = 0.4$ (Gregg & Sing, 1982).

The α_s plots for several alginate, alginic acid and κ -carrageenan aerogels are reported in Fig. 5. The slopes of the plots largely differ, corresponding to surface areas spanning from $130 \text{ m}^2 \text{ g}^{-1}$ for a κ -carrageenan aerogel to $680 \text{ m}^2 \text{ g}^{-1}$ for a copper alginate aerogel. The difference in surface area depends both on the preparation of the parent hydrogel and on the effectiveness of the supercritical drying procedure. Despite their different slopes, all plots present a common feature: their extrapolation crosses the volume axis at a

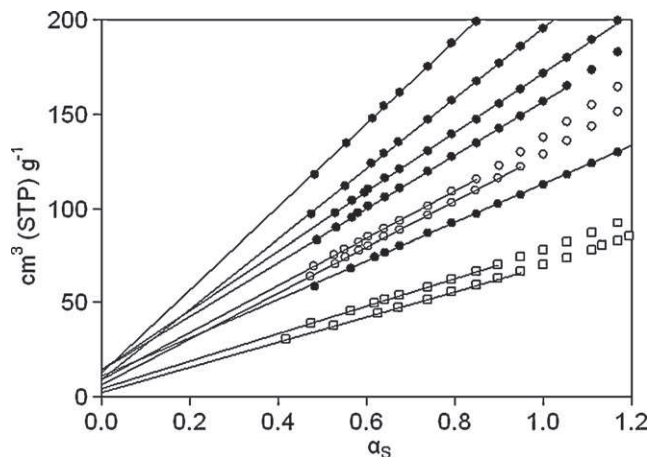


Fig. 5. Comparison plots of the adsorption of N_2 at 77 K on (filled circles) ionotropic alginate, (void circles) alginic acid, and (void squares) carrageenan aerogels. The lines represent best-fit linear correlations.

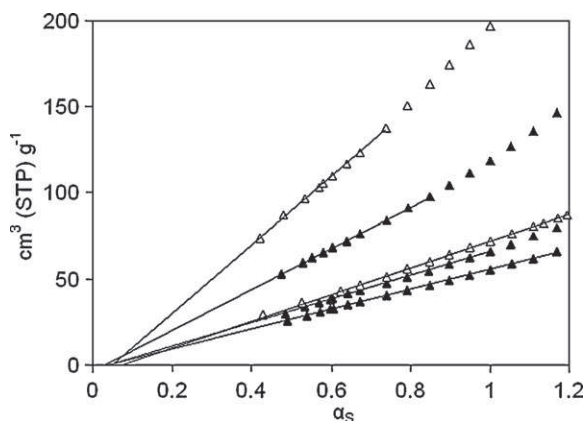


Fig. 6. Comparison plots of the adsorption of N_2 at 77 K on (filled triangles) chitosan and (void triangles) chitin aerogels. The lines represent best-fit linear correlations.

positive value (the volume values are given as volume of adsorbed gas at standard temperature and pressure, STP). The positive intercept corresponds to a larger-than-expected adsorbed volume at low pressure, which corresponds to a more energetic adsorption than on the reference silica adsorbent. The higher adsorption enthalpy can depend either on the texture or the composition of the surface. In the first case, a molecule is surrounded by the surface of a micropore and interacts with a larger number of surface sites. In the second case, the presence of strong adsorption sites justifies the higher adsorption at low pressure.

The α_5 plots for several chitosan and chitin aerogels are reported in Fig. 6. The slope of the plots varies according to the surface of the aerogels, from $150 \text{ m}^2 \text{ g}^{-1}$ for the worse chitosan aerogel to $560 \text{ m}^2 \text{ g}^{-1}$ for the best chitin aerogel. In all cases, the extrapolation of the plots crosses the volume axis at negative values. In the case of agar aerogels, the ordinates at $\alpha_5 = 0$ presented positive or negative values very close to zero (not represented).

A negative value of the intercept indicates a lower-than-expected adsorbed volume at low pressure and is less common than a positive one. It can only be interpreted by admitting that the energy of adsorption of N_2 is lower on the measured solid than on the reference adsorbent, silica in our case. This brings about a lower density of the adsorbed monolayer (Day, Parfitt, & Peacock, 1979; Lovell, 1975) and a decrease of the amount of N_2 adsorbed in the monolayer by comparison with the value that would have been adsorbed on a silica surface with the same surface area as the examined sample. As a consequence, the α_5 plot presents a negative intercept at the origin. The part of the α_5 plot beyond the monolayer is virtually unaffected by the density of the monolayer, as the influence of the nature of the adsorbent is especially important for adsorbed molecules in direct contact with the surface. When more than a monolayer has been adsorbed, further adsorption takes place through adsorbate-to-adsorbate interactions and the correlation between relative pressure and adsorbed amount is scantily modified by the nature of the underlying surface. In this way, the deviation from linearity of the low-pressure part of the α_5 plot can be correlated the energy of adsorption on the surface.

The BET treatment provides an energetic parameter $C(\text{BET})$, which allows to evaluate the net molar energy of adsorption ΔE , viz. the difference between the adsorption enthalpy in the monolayer and in further layers. The net energy of adsorption ΔE is reported in Fig. 7 for all samples as a function of the extrapolated volume at $\alpha_5 = 0$, which quantifies the variations of density of the adsorbed monolayer from the density of the monolayer adsorbed on the reference silica.

The net adsorption energy ΔE is fairly proportional to the variation of density of the adsorbed monolayer. The absolute values can

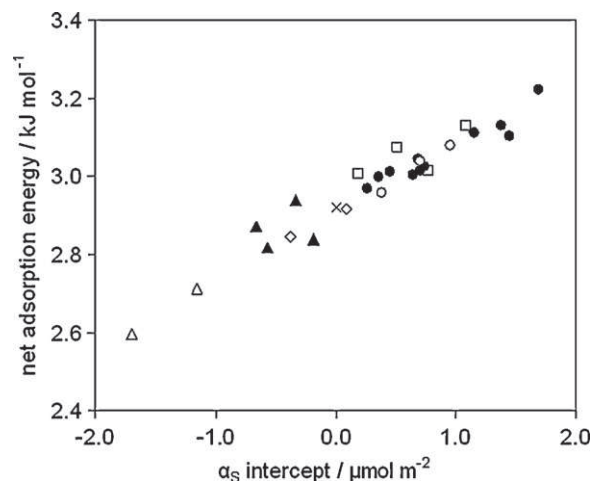


Fig. 7. Net molar energy of adsorption of N_2 vs. the intercept at $\alpha_5 = 0$ (Figs. 5 and 6) for chitin (void triangles), chitosan (filled triangles), agar (void lozenges), carrageenan (void square), alginic acid (void circles), and alginate (filled circles) aerogels and (St. Andrews' cross) fumed silica.

be compared with the net adsorption energy measured on amorphous silica, which value, 2.9 kJ mol^{-1} , is in good agreement with literature results (Lefebvre & Jolicoeur, 1992). In the case of the aerogels of alginate, alginic acid, and carrageenan, ΔE is always higher than the value measured on the reference silica. For chitosan and agar aerogels, ΔE is slightly lower than for silica. ΔE of chitin aerogel is much lower than the silica's one.

4. Discussion

4.1. Factors affecting the texture of the aerogels

The surface area of the aerogel can bring a reliable information about the size of the secondary units which form the polymer network, provided that the shape of the aggregates and the density of the polymer can be reasonably assessed by independent techniques. It would be obviously interesting to determine if this information on the aerogel could be used to desume properties of the parent hydrogel. In some cases, a good retention of the structure of the hydrogel in the supercritically dried aerogel has been demonstrated. In the case of Ca-alginate, SAXS studies have shown that the aerogel retains the fibrillar structure of the hydrogel (Robitzer et al., 2008). The hydrogel presented a well-defined rod-like morphology and this shape was retained through the solvent exchanges and the supercritical drying treatment.

However, other polysaccharides do not always present the level of stability of alginate gels. Solvent exchanges and modification of physical conditions involved in the supercritical drying treatment can alter in several ways the texture of the gel. The degree of shrinkage of the gel and the formation of mesoporosity are good indicators of such modifications.

The shrinkage of a fibrillar gel can take place according to several mechanisms, originated by different driving forces. In Fig. 8, two major alternative mechanisms of shrinkage of a bidimensional network of rigid rods are schematically represented. Shrinkage can take place independently of drying, when a change of solvent from water to a less interacting solvent provides the driving force for a decrease of the surface/volume ratio of the polymer aggregates. In the case of fibrillar aggregates, a lower affinity for the solvent corresponds to a potential for thickening and shortening of the fibrils. If the solvent is a good plasticizer, as ethanol and CO_2 can be for several polymers (Tsivintzelis, Pavlidou, & Panayotou, 2007), the reorganization of polysaccharide chains to form thicker fib-

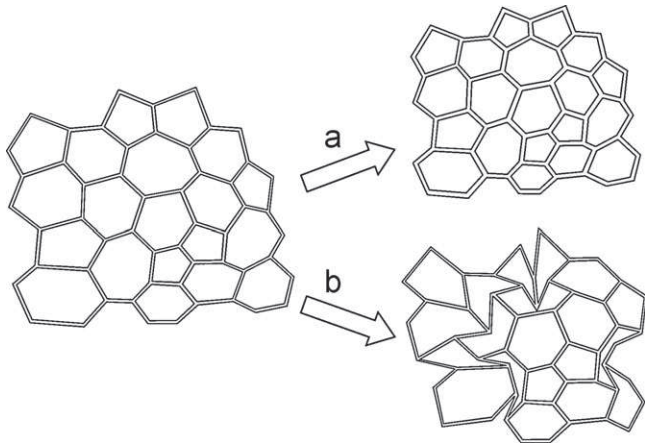


Fig. 8. Schematic representation of alternative mechanisms of shrinkage of a fibrillar gel: (a) homothetic shrinkage by fibril thickening and (b) non-homogeneous shrinkage by local collapses.

rils can occur in a reasonably short time and the corresponding shortening of fibrils induces a homothetic shrinkage of the gel, as depicted in the path A of Fig. 8. This mechanism uniformly decreases the size of the cavities among fibrils. In the case of macroporous hydrogels with cavities of several hundreds nanometers, shrinkage by decreased solvent affinity is unlikely to generate cavities small enough to enter in the domain of mesoporosity and be measured by N_2 physisorption. Such a mechanism is probably at the origin of the texture of the aerogels of agar and chitosan from β -chitin, which did undergo a significant shrinkage but do not present any significant mesoporosity. The formation of larger structures when water is replaced by alcohol has been observed for several gelling systems of polysaccharides, as in the cases of squid-pen chitosan (Boucard, Viton, & Domard, 2005) and guar (Gittings et al., 2001).

A different mechanism is operating when interface tension is the driving force for shrinkage. Gas-liquid interfaces are expected to be eliminated in supercritical drying. However, incomplete solvent exchange can lead to local retention of solvents with a critical point higher than CO_2 and to the formation of gas-liquid interfaces when supercritical CO_2 is extracted. In this case, interface tension can draw together fibrils from the opposite sides of a cavity. The net results are global shrinkage of the gel and local formation of a porosity much smaller than the original one. The collapse of cavities is unlikely to be an homogeneous phenomenon, especially because water or alcohol retention is more likely in the smallest cavities and in the core of the gel. Moreover, the resistance of the network to interface tension follows a complex pattern, in which the higher interface tension in smaller cavities is partially compensated by the lower mechanical stiffness of networks with larger cavities (Gibson & Ashby, 1997). The collapse of the weakest points of the network brings about a non-uniform shrinkage of the gel, as schematically represented in the path B of Fig. 8. Such a mechanism probably accounts for most cases of formation of mesoporosity in otherwise macroporous gels, as observed for most of the aerogels whose textural properties are reported in Table 1. In the schematic representation of Fig. 8, fibrils are represented by rigid rods and the connectivity of the network is assumed not to be affected by shrinkage. In a real gel, fibrils can be quite flexible and nodes can be shredded by severe stress. Both factors contribute to decrease the resilience of the network and allow a generalized collapse of the gel. The severe shrinkage of κ -carrageenan gel in the supercritical drying treatment is an interesting example of uniform collapse, in which the macroporosity of the hydrogel is shrunk to a mesoporosity with a narrow pore size distribution.

A critical parameter for the stiffness of the fibrils is the temperature of glass transition (T_g) of the polymer they are formed of. Beyond representing a practical limit to the thermal stability of the porosity, T_g can also affect the behaviour of the gel in the drying process. The T_g of polysaccharides is strongly related to their molecular weight, to the gelling mechanism and the moisture content. Ionotropic gelling by divalent cations increases the T_g of alginate from 80 to 130 °C (Mruthyunjaya Swamy, Ramaraj, & Siddaramaiah, 2010; Russo, Malinconico, & Santagata, 2007) and T_g as high as 200 °C have been suggested for chitin and chitosan (Matsui, Munaro, & Akcelrud, 2010; Sakurai, Maegawa, & Takahashi, 2000). T_g is significantly increased by the drying treatment: in the case of some agar gels a decrease of the water content from 15 to 1% brings about an increase of T_g from 60 to 125 °C (Mitsuiki, Mizuno, & Motoki, 1999). At difference with other polysaccharides, κ -carrageenan presents a very low T_g , about 1 °C for 12% water content. The corresponding plasticity at room temperature probably accounts for the observed deformation of carrageenan gel in the intermediate steps of the drying process.

Anyway, the extreme example of shrinkage is observed in evaporative drying, in which the full force of the water-vapour interface is exerted on the network. In these cases, the fibrils coalesce in a compact solid and no porosity can be observed on the polysaccharide xerogels formed by such a drying method (Di Renzo et al., 2005; Valentin et al., 2007).

4.2. Correlations among surface energetics, monolayer density, and polymer polarity

The shape of the physisorption isotherm at low relative pressure provides information on the affinity of the adsorbate for the surface. The $C(BET)$ parameter and the low-coverage variations of the slope of the comparison plots are both related to the shape of the initial part of the adsorption isotherm and provide an information on the energy of adsorption. A possible trouble in the interpretation of these data is the effect of the presence of any microporosity, which would increase the energy of adsorption independently of the chemical nature of the surface.

When the comparison plots of the polysaccharide aerogels are considered (Figs. 5 and 6), the presence of micropores would be a tempting explanation of the positive intercept of the α_5 plots for alginates and carrageenan. However, the energetics of low-pressure adsorption can be affected in a very similar way by the presence of strong adsorption sites on the surface. Quite high $C(BET)$ values can either be justified by a strong interaction between adsorbent and adsorbate or by the presence of a limited volume of micropores or surface roughness.

The negative intercept of the α_5 plots for chitin and chitosan could be accounted for by the geometry of the surface only if some microporosity was present in the standard adsorbent used. If some microporosity is commonly observed in precipitated silica, the use of a fumed silica standard adsorbent at low relative pressure allow to avoid the inconveniences related to the presence of micropores (Carrott, Roberts, & Sing, 1988). The negative intercepts observed for chitin and chitosan can rather be justified by an energy of adsorption lower than the energy of adsorption on the fumed silica used as standard for the α_5 method. Lower $C(BET)$ parameters have been shown to correspond to a larger surface area covered by an adsorbed N_2 molecule. For instance, an increase of molecular areas of 24% was measured on a reference silica when a hydrocarbon coating lowered the $C(BET)$ parameter at a value of 12 (Jelinek & Kováts, 1994). This effect was attributed to a different orientation of the N_2 molecules on the surface. On a non-polar surface, the N_2 molecules are quite flat on the surface and tend to occupy the maximum area. On a polar surface, the quadrupolar moment of the

N₂ molecule favours a head-on adsorption, with the formation of a denser monolayer (Trens, Denoyel, & Glez, 2004). In the case of the chitin and chitosan aerogels, a lower density of the N₂ monolayer is a sensible explanation of the lower-than-expected adsorbed volume at low pressure, hence the negative intercept of the α_5 plot.

The observed order of the energies of adsorption of N₂ on the different polysaccharides is alginate ~ alginic acid \geq carrageenan > agar ~ chitosan > chitin. This ranking is in good agreement with the order of polarity of the polymers, which can be evaluated from the octane/water partition coefficient of the monomers. Indeed, the calculated partition coefficients decrease from -0.71 for chitin to -1.85 for chitosan, -2.30 for agar, and -2.60 for alginic acid, the higher values corresponding to less polar substances (Ghose, Pritchett, & Crippen, 1989). It can be observed that the polarity of molecules as evaluated by their octane/water partition coefficient often differ from the polarity of the corresponding surfaces as evaluated by another widely used method, the measurement of the contact angles of water. The values of the advancing and receding contact angles are affected by several parameters related to the preparation of the sample and the experimental setting (Barthlott & Neinhuis, 1997; Gao, McCarthy, & Zhang, 2009; Lam, Wu, Li, Hair, & Neumann, 2002). Among these factors, the most important is probably the topology of the surface at the micron scale, as surface roughness is expected to enhance hydrophilic and hydrophobic properties at an enormous extent (Cassie & Baxter, 1944; Koch, Bohn, & Barthlott, 2009; Onda, Shibuichi, Satoh, & Tsujii, 1996). Variations of surface topology can account for most of the wide scattering of experimental contact angles measured on polysaccharide surfaces (Cunha & Gandini, 2010; Yasuda & Okuno, 1994). For instance, water contact angle varying from 13° (superhydrophilic) to 103° (highly hydrophobic) have been measured on chitosan surfaces (Silva et al., 2007; Wang, Fang, & Yan, 2001). The contact angle provides information on the energy of interaction of a macroscopic object, like a water droplet or a cell, with a macroscopic polymer surface, at a scale much larger than the physisorption of a probe molecule with individual surface sites.

The variation of physisorption energy of N₂ with the polarity of the polymer implies that the functional groups of the polymers are accessible at the surface of the aerogel fibrils. Indeed, the main factor affecting polymer polarity and adsorption energetics is the nature of the functional groups of the polysaccharide, viz. carboxylates of divalent cations for the alginates, carboxylic groups for the alginic acid, sulphonic groups for carrageenan, hydroxy groups alone for agar, amino groups for chitosan, and acetylamido groups for chitin. The presence of electron-deficient metal cations or acidic protons induces higher adsorption energy than on fumed silica, while the organic protection of the acetylated groups of chitin induces much lower adsorption energy than on fumed silica. The functional groups of the agar gel are hydroxy groups, which behave in a similar way as the silanols of the silica surface. Indeed, the N₂ adsorption energy and the intercept of the α_5 -plot for agar and silica are virtually identical. The relatively low polarity of the chitosan surface is in good agreement with the observation of a relative hydrophobicity of the chitosan gels (Boucard et al., 2007; Montembault, Viton, & Domard, 2005).

The alginate aerogels examined covered a wide range of composition, both from the point of view of the guluronic/mannuronic ratio and of the nature of the compensating cation. No significant correlations were found between these parameters and the energy of adsorption. Indeed, also alginic acid presents a N₂ adsorption energy in the same range as the alginates salted by transition metal cations. Alginic acid has been shown to present a distance between OH groups compatible with adsorption of polar molecules, like

water and alcohols, by interaction with a couple of neighbouring sites (Rodriguez Escudero, Robitzer, Di Renzo, & Quignard, 2009). The higher interaction energy by comparison with silica parallels the higher acidity of the carboxylic groups by comparison with silanol.

The correlation between energetics of N₂ adsorption and polarity of the surface has a quite general value and also applies to synthetic polymers. If a C(BET) parameter is evaluated from published adsorption isotherms and the net physisorption energy ΔE is calculated from this parameter, ΔE as low as 1.8 kJ mol⁻¹ can be calculated for hydrophobic polystyrene (Davankov & Tsyurupa, 1989) and as high as 3.1 kJ mol⁻¹ for more polar melamine-formaldehyde resin (Derylo-Marczewska, Goworek, & Zgrajka, 2001). However, it has always to be taken into account that a high adsorption energy can either be attributed to the presence of strong adsorption sites or to the presence of micropores. An independent assessment of the chemistry of the surface is needed to differentiate among the two possible explanations. For instance, the measurement of ΔE as high as 3 kJ mol⁻¹ for hydrophobic polymers like polystyrene (Milano et al., 2001) or poly(styrene-butadiene) (Deleuzel, Schultze, & Sherrington, 2000) has logically been attributed to the presence of micropores.

5. Conclusions

Physisorption is the only technique able to provide quantitative information on the surface area and the mesoporosity of polysaccharide aerogels. However, full understanding of the texture of a material requires the synergy of several techniques. Electron microscopy provides local information on the shape and the size of the secondary structures of the material. This information is useful to choose the proper model for the interpretation of the physisorption data. On the other way, the physisorption measurement of the property of the whole sample usefully complements the local nature of the data from microscopy. The limitation of the data from capillary condensation to features smaller than 50 nm has always to be taken into account, and the evaluation of macroporosity has to be provided by macroscopic techniques.

The texture of the aerogel can provide information on the gelling mechanism and on the evolution of the material in the drying process. Data on the macroscopic shrinkage of the gel in the drying process allows to differentiate between systems for which the aerogel provides a faithful image of the parent hydrogel and systems with low mechanical stability. The extent of shrinkage provides a qualitative information on the stiffness of the secondary structures and physisorption data provide a quantitative information on their coalescence.

The high surface area of the aerogels renders much easier the evaluation of the surface properties of the polymers by any technique. The adsorption of probe molecules, monitored by spectroscopic, volumetric or calorimetric methods, provides an important information on the accessibility of the functional groups of the polymer. The different values of the adsorption heat for polymers with different functional groups indicate that the versatile chemistry of polysaccharides can be used to prepare materials which retain their specific properties also in the dry state. In the case of natural materials, physisorption methods are a promising tool to identify the functional groups exposed to the surface of complex systems, as it has just been suggested by recent research on lignocellulosic systems (Chang et al., 2009; Clair, Gril, Di Renzo, Yamamoto, & Quignard, 2008).

References

- Absolom, D. R., Lamberti, F. V., Policova, Z., Sing, W., van Oss, C. J., & Neumann, A. W. (1983). Surface thermodynamics aspects of bacterial adhesion. *Applied and Environmental Microbiology*, 46, 90–97.

- Aronson, M., Medalia, O., Schori, L., Mirelman, D., Sharon, N., & Ofek, I. (1979). Prevention of colonization of the urinary tract of mice with *Escherichia coli* by blocking of bacterial adherence with methyl α -D-mannopyranoside. *Journal of Infectious Diseases*, 139, 329–332.
- Atkins, E. D. T., Nieduszynski, I. A., Mackie, W., Parker, K. D., & Smolko, E. E. (1973). Structural components of alginic acid. II. The crystalline structure of poly- α -L-guluronic acid. Results of X-ray diffraction and polarized infrared studies. *Biopolymers*, 12, 1879–1887.
- Barthlott, W., & Neinhuis, C. (1997). Purity of the sacred lotus, or escape from contamination in biological surfaces. *Planta*, 202, 1–8.
- Bayer, M. E. (1990). Visualization of the bacterial polysaccharide capsule. In J. Kann, & B. Kann (Eds.), *Bacterial capsules* (pp. 129–157). Berlin: Springer-Verlag.
- Boissière, M., Tourrette, A., Devoisselle, J. M., Di Renzo, F., & Quignard, F. (2006). Pillaring effects in macroporous carraegenan–silica composite microspheres. *Journal of Colloid and Interface Science*, 294, 109–116.
- Boucard, N., David, L., Rochas, C., Montembault, A., Viton, C., & Domard, A. (2007). Polyelectrolyte microstructure in chitosan aqueous and alcohol solutions. *Biomacromolecules*, 8, 1209–1217.
- Boucard, N., Viton, C., & Domard, A. (2005). New aspects of the formation of physical hydrogels of chitosan in a hydroalcoholic medium. *Biomacromolecules*, 6, 3227–3237.
- Cardea, S., Gugliuzza, A., Sessa, M., Aceto, M. C., Drioli, E., & Reverchon, E. (2009). Supercritical gel drying: A powerful tool for tailoring symmetric porous PVDF-HFP membranes. *ACS Applied Materials and Interfaces*, 1, 171–180.
- Carrott, P. J. M., Roberts, R. A., & Sing, K. S. W. (1988). Adsorption of neopentane by nonporous carbons and silicas. *Langmuir*, 4, 740–743.
- Cassie, A. B. D., & Baxter, S. (1944). Wettability of porous surfaces. *Transactions of the Faraday Society*, 40, 546–551.
- Casson, D., & Emery, A. N. (1987). On the elimination of artefactual effects in assessing the structure of calcium alginate cell immobilization gels. *Enzyme and Microbial Technology*, 9, 102–106.
- Chang, S.-S., Clair, B., Ruelle, J., Beauchêne, J., Di Renzo, F., Quignard, F., et al. (2009). Mesoporosity as a new parameter for understanding tension stress generation in trees. *Journal of Experimental Botany*, 60, 3023–3030.
- Chang, X., Chen, D., & Jiao, X. (2008). Chitosan-based aerogels with high adsorption performance. *Journal of Physical Chemistry B*, 112, 7721–7725.
- Chassary, P., Vincent, T., & Guibal, E. (2004). Metal anion sorption on chitosan and derivative materials: A strategy for polymer modification and optimum use. *Journal of Applied Polymer Science*, 94, 1634–1642.
- Cherstvy, A. G., Kolomeisky, A. B., & Kornyshev, A. A. (2008). Protein–DNA interactions: Reaching and recognizing the targets. *Journal of Physical Chemistry B*, 112, 4741–4750.
- Chu, Y.-F., Hsu, C.-H., Soma, P. K., & Lo, Y. M. (2009). Immobilization of bioluminescent *Escherichia coli* cells using natural and artificial fibers treated with polyethyleneimine. *Bioresource Technology*, 101, 3167–3174.
- Clair, B., Gril, J., Di Renzo, F., Yamamoto, H., & Quignard, F. (2008). Characterisation of a gel in the cell walls to elucidate the paradoxical shrinkage of tension wood. *Biomacromolecules*, 9, 494–498.
- Cunha, A. G., & Gandini, A. (2010). Turning polysaccharides into hydrophobic materials: A critical review. Part 2. Hemicelluloses, chitin/chitosan, starch, pectin and alginates. *Cellulose*, 17, 1045–1065.
- Daniel, C., Alfano, D., Venditto, V., Cardea, S., Reverchon, E., Larobina, D., et al. (2005). Aerogels with a microporous crystalline host phase. *Advanced Materials*, 17, 1515–1518.
- Davankov, V. A., & Tsyurupa, M. P. (1989). Structure and properties of porous hypercrosslinked polystyrene sorbents 'Styrosorb'. *Pure & Applied Chemistry*, 61, 1881–1888.
- Day, R. E., Parfitt, G. D., & Peacock, J. (1979). A comparison of the effect of pre-treatment with ethanol, hexan-1-ol, and hexan-1:6-diol on the adsorption behavior of rutile, alumina, and silica. *Journal of Colloid and Interface Science*, 70, 130–138.
- Decho, A. W. (1999). Imaging an alginate polymer gel matrix using atomic force microscopy. *Carbohydrate Research*, 315, 330–333.
- Deleuzel, H., Schultze, X., & Sherrington, D. C. (2000). Porosity analysis of some poly(styrene/divinylbenzene) beads by nitrogen sorption and mercury intrusion porosimetry. *Polymer Bulletin*, 44, 179–186.
- Derylo-Marczewska, A., Goworek, J., & Zgrajka, W. (2001). Studies of melamine–formaldehyde resins by sorption from gas and liquid phases. *Langmuir*, 17, 6518–6523.
- Dhoot, N. O., & Wheatley, M. A. (2003). Microencapsulated liposomes in controlled drug delivery: Strategies to modulate drug release and eliminate the burst effect. *Journal of Pharmaceutical Sciences*, 92, 679–689.
- Di Renzo, F., Valentini, R., Boissière, M., Tourrette, A., Sparapano, G., Molvinger, K., et al. (2005). Hierarchical macroporosity induced by constrained syneresis in core–shell polysaccharide composites. *Chemistry of Materials*, 17, 4693–4699.
- Disney, M. D., Zheng, Z., Swager, T. M., & Seeberger, P. H. (2004). Detection of bacteria with carbohydrate-functionalized fluorescent polymers. *Journal of the American Chemical Society*, 126, 13343–13346.
- Drury, J. L., & Mooney, D. J. (2003). Hydrogels for tissue engineering: Scaffold design variables and applications. *Biomaterials*, 24, 4337–4351.
- Dumitriu, S. (Ed.). (1998). *Polysaccharides*. New York: Marcel Dekker.
- Dumitriu, S., & Chornet, E. (1998). Polysaccharides as support for enzyme and cell immobilization. In S. Dumitriu (Ed.), *Polysaccharides* (pp. 629–748). New York: Marcel Dekker.
- Elbert, D. L., & Hubbell, J. A. (1996). Surface treatments of polymers for biocompatibility. *Annual Review of Material Research*, 26, 365–394.
- Foord, S. A., & Atkins, E. D. T. (1989). New X-ray-diffraction results from agarose extended single helix structures and implications for gelation mechanism. *Biopolymers*, 28, 1345–1365.
- Galarneau, A., Desplandier, D., Dutartre, R., & Di Renzo, F. (1999). Micelle-templated silicas as a test-bed for methods of pore size evaluation. *Microporous and Mesoporous Materials*, 27, 297–308.
- Gao, L., McCarthy, T. J., & Zhang, X. (2009). Wetting and superhydrophobicity. *Langmuir*, 25, 14100–14104.
- Ghose, A. K., Pritchett, A., & Crippen, G. M. (1989). Atomic physicochemical parameters for three dimensional structure directed quantitative structure–activity relationship. III. Modeling hydrophobic interactions. *Journal of Computational Chemistry*, 9, 80–90.
- Gibson, L. J., & Ashby, M. F. (1997). *Cellular Solids. Structure and Properties*. Cambridge: Cambridge University Press.
- Gittings, M. R., Cipelletti, L., Trappe, V., Weitz, D. A., In, M., & Lal, J. (2001). The effect of solvent and ions on the structure and rheological properties of guar solutions. *Journal of Physical Chemistry A*, 105, 9310–9315.
- Gregg, S. J., & Sing, K. S. W. (1982). *Adsorption, Surface area and Porosity* (2nd ed.). London: Academic Press. (p. 98).
- Guibal, E. (2005). Heterogeneous catalysis on chitosan-based materials: A review. *Progress in Polymer Science*, 30, 71–109.
- Guibal, E., Vincent, T., & Peirano-Blondet, F. (2007). Biopolymers as supports for heterogeneous catalysis: Focus on chitosan, a promising aminopolysaccharide. In A. K. S. Gupta (Ed.), *Ion Exchange and Solvent Extraction* (p. 151–290). Boca Raton: CRC Press.
- Hills, B. P., Godward, J., Debatty, M., Barras, L., Saturio, C. P., & Ouwerx, C. (2000). NMR studies of calcium induced alginate gelation. Part II. The internal bead structure. *Magnetic Resonance in Chemistry*, 38, 719–728.
- Jaafari, K., Elmaleh, S., Coma, J., & Benkhouja, K. (2001). Equilibrium and kinetics of nitrate removal by protonated cross-linked chitosan. *Water SA*, 27, 9–13.
- Jaroniec, M., Kruk, M., & Olivier, J. P. (1999). Standard nitrogen adsorption data for characterization of nanoporous silicas. *Langmuir*, 15, 5410–5413.
- Jelinek, L., & Kováts, E. S. Z. (1994). True surface areas from nitrogen adsorption experiments. *Langmuir*, 10, 4225–4231.
- Kanzawa, Y., Koreeda, A., Harada, A., & Harada, T. (1989). Electron microscopy of the gel-forming ability of polysaccharide food additives. *Agricultural and Biological Chemistry*, 53, 979–986.
- Kanzawa, Y., Koreeda, A., Harada, A., Okuyama, K., & Harada, T. (1990). Significance of molecular association for polysaccharide gels in food. *Journal of Home Economics of Japan*, 41, 951–956.
- Koch, K., Bohn, H. F., & Barthlott, W. (2009). Hierarchically sculptured plant surfaces and superhydrophobicity. *Langmuir*, 25, 14116–14120.
- Kopecká, M., Phaff, H. J., & Fleet, G. H. (1974). Demonstration of a fibrillar component in cell wall of yeast *Saccharomyces cerevisiae* and its chemical nature. *Journal of Cell Biology*, 62, 66–76.
- Lam, C. N. C., Wu, R., Li, D., Hair, M. L., & Neumann, A. W. (2002). Study of the advancing and receding contact angles: Liquid sorption as a cause of contact angle hysteresis. *Advances in Colloid and Interface Science*, 96, 169–191.
- Lamarque, G., Viton, C., & Domard, A. (2004). Comparative study of the first heterogeneous deacetylation of α - and β -chitins in a multistep process. 5, 992–1001.
- Laus, R., Geremias, R., Vasconcelos, H. L., Laranjeira, M. C. M., & Fávère, V. T. (2007). Reduction of acidity and removal of metal ions from coal mining effluents using chitosan microspheres. *Journal of Hazardous Materials*, 149, 471–474.
- Leckband, D. (2001). Novel recognition mechanisms in biological adhesion. *Current Opinion in Colloid & Interface Science*, 6, 498–505.
- Lee, J.-H., Shim, J. S., Lee, J. S., Kim, J. K., Yang, I. S., Chung, M.-S., et al. (2006). Inhibition of pathogenic bacterial adhesion by acidic polysaccharide from green tea (*Camellia sinensis*). *Journal of Agricultural and Food Chemistry*, 54, 8717–8723.
- Lefebvre, Y., & Jolicoeur, C. (1992). Gas phase adsorption studies of selected probe molecules on powdered silica polymorphs. *Colloids and Surfaces*, 63, 67–76.
- Li, B., & Logan, B. E. (2004). Bacterial adhesion to glass and metal-oxide surfaces. *Colloids and Surfaces B-Biointerfaces*, 36, 81–90.
- Lippens, B. C., & de Boer, J. H. (1965). Studies on pore systems in catalysts. V. The t method. *Journal of Catalysis*, 4, 319–323.
- Liu, Z. M., Becker, T., & Neufeld, R. J. (2005). Spherical alginate granules formulated for quick-release active subtilisin. *Biotechnology Progress*, 21, 568–574.
- Liu, Y., Yang, C.-H., & Li, J. (2007). Influence of extracellular polymeric substances on *Pseudomonas aeruginosa* transport and deposition profiles in porous media. *Environmental Science and Technology*, 41, 198–205.
- Lovell, V. M. (1975). The effect of certain pretreatments on surface-area of various minerals, determined by BET method. *Powder Technology*, 12, 71–76.
- Mackie, W., Perez, S., Rizzo, R., Taravel, F., & Vignon, M. (1983). Aspects of the conformation of polyguluronate in the solid state and in solution. *International Journal of Biological Macromolecules*, 5, 329–341.
- Mammen, N., Choi, A.-K., & Whitesides, G. M. (1998). Polyvalent interactions in biological systems: Implications for design and use of multivalent ligands and inhibitors. *Angewandte Chemie-International Edition*, 37, 2754–2794.
- Martinsen, A., Storø, I., & Skjåk-Bræk, G. (1992). Alginate as immobilization material. 3. Diffusional properties. *Biotechnology and Bioengineering*, 39, 186–194.
- Matsui, M., Munaro, M., & Akcelrud, L. (2010). Chitin/polyurethane blends: A thermal and morphological study. *Polymer International*, 59, 1090–1098.
- Maurstad, G., Danielsen, S., & Stokke, B. T. (2003). Analysis of compacted semiflexible polyanions visualized by atomic force microscopy: Influence of chain stiffness on the morphologies of polyelectrolyte complexes. *Journal of Physical Chemistry B*, 107, 8172–8180.

- Milano, G., Venditto, V., Guerra, G., Cavallo, L., Ciambelli, P., & Sannino, D. (2001). Shape and volume of cavities in thermoplastic molecular sieves based on syndiotactic polystyrene. *Chemistry of Materials*, 13, 1506–1511.
- Millane, R. P., Chandrasekaran, R., Arnott, S., & Dea, I. C. M. (1988). The molecular structure of κ -carrageenan and comparison with λ -carrageenan. *Carbohydrate Research*, 182, 1–17.
- Mitsuiki, M., Mizuno, A., & Motoki, M. (1999). Determination of molecular weight of agars and effect of the molecular weight on the glass transition. *Journal of Agricultural and Food Chemistry*, 47, 473–478.
- Miura, Y., Watanabe, Y., & Okabe, S. (2007). Membrane biofouling in pilot-scale membrane bioreactors (MBRs) treating municipal wastewater: Impact of biofilm formation. *Environmental Science & Technology*, 41, 632–638.
- Montebault, A., Viton, C., & Domard, A. (2005). Physico-chemical studies of the gelation of chitosan in a hydroalcoholic medium. *Biomaterials*, 26, 933–943.
- Murthyunajaya Swamy, T. M., Ramaraj, B., & Siddaramaiah. (2010). Sodium alginate and poly(ethylene glycol) blends: Thermal and morphological behaviors. *Journal of Macromolecular Science A*, 47, 877–881.
- Neimark, A. V. G., & Ravikovitch, P. I. (2001). Capillary condensation in MMS and pore structure characterization. *Microporous and Mesoporous Materials*, 44, 697–707.
- Neville, A. C., Parry, D. A. D., & Woodhead-Galloway, J. (1976). The chitin crystallite in arthropod cuticle. *Journal of Cell Science*, 21, 73–82.
- Okuyama, K., Noguchi, K., Miyazawa, T., Yui, T., & Ogawa, K. (1997). Molecular and crystal structure of hydrated chitosan. *Macromolecules*, 30, 5849–5855.
- Onda, T., Shibuichi, S., Satoh, N., & Tsujii, K. (1996). Super-water-repellent fractal surfaces. *Langmuir*, 12, 2125–2127.
- Partap, S., Rehman, I., Jones, J. R., & Darr, J. A. (2006). “Supercritical carbon dioxide in water” emulsion-templated synthesis of porous calcium alginate hydrogels. *Advanced Materials*, 18, 501–504.
- Pekala, R. W. (1989). Organic aerogels from the polycondensation of resorcinol with formaldehyde. *Journal of Materials Science*, 24, 3221–3227.
- Peppas, N. A., Hilt, J. Z., Khademhosseini, A., & Langer, R. H. (2006). Hydrogels in biology and medicine: From molecular principles to bionanotechnology. *Advanced Materials*, 18, 1345–1360.
- Percival, E., & McDowell, R. H. (1967). *Chemistry and enzymology of marine algal polysaccharides*. London: Academic Press. (p. 23).
- Pierre, A. C., & Pajonk, G. M. (2002). Chemistry of aerogels and their applications. *Chemical Reviews*, 102, 4243–4265.
- Pilnik, W., & Rombouts, F. M. (1985). Polysaccharides and food processing. *Carbohydrate Research*, 142, 93–105.
- Quignard, F., Valentin, R., & Di Renzo, F. (2008). Aerogel materials from marine polysaccharides. *New Journal of Chemistry*, 32, 1300–1310.
- Ravi Kumar, M. V. N., Muzzarelli, R. A. A., Sashiwa, H., & Domb, A. J. (2004). Chitosan chemistry and pharmaceutical perspectives. *Chemical Reviews*, 104, 6017–6084.
- Roberts, G. A. F. (1992). *Chitin chemistry*. Houndmills: Macmillan.
- Robitzer, M., David, L., Rochas, C., Di Renzo, F., & Quignard, F. (2008). Nanostructure of calcium alginate aerogels obtained from multistep solvent exchange route. *Langmuir*, 24, 12547–12552.
- Rodríguez Escudero, R., Robitzer, M., Di Renzo, F., & Quignard, F. (2009). Alginate aerogels as adsorbents of polar molecules from liquid hydrocarbons. Hexanol as probe molecule. *Carbohydrate Polymers*, 75, 52–57.
- Rouquerol, F., Rouquerol, J., & Sing, K. S. W. (1999). *Adsorption by powders and porous solids*. San Diego: Academic Press.
- Russo, R., Malinconico, M., & Santagata, G. (2007). Effect of cross-linking with calcium ions on the physical properties of alginate films. *Biomacromolecules*, 8, 3193–3197.
- Sadamoto, R., Niikura, K., Ueda, T., Monde, K., Fukuhara, N., & Nishimura, S.-I. (2004). Control of bacteria adhesion by cell-wall engineering. *Journal of the American Chemical Society*, 126, 3755–3761.
- Sakurai, K., Maegawa, T., & Takahashi, T. (2000). Glass transition temperature of chitosan and miscibility of chitosan/poly(N-vinyl pyrrolidone) blends. *Polymer*, 41, 7051–7056.
- Schengrund, C.-L. (2003). “Multivalent” saccharides: Development of new approaches for inhibiting the effects of glycosphingolipid-binding pathogens. *Biochemical Pharmacology*, 65, 699–707.
- Serp, D., Mueller, M., von Stockar, U., & Marison, I. W. (2002a). Low-temperature electron microscopy for the study of polysaccharide ultrastructures in hydrogels. I. Theoretical and technical considerations. *Biotechnology and Bioengineering*, 79, 243–252.
- Serp, D., Mueller, M., von Stockar, U., & Marison, I. W. (2002b). Low-temperature electron microscopy for the study of polysaccharide ultrastructures in hydrogels. II. Effect of temperature on the structure of Ca^{2+} -alginate beads. *Biotechnology and Bioengineering*, 79, 253–259.
- Sharon, N., & Ofek, B. (2000). Safe as mother’s milk: Carbohydrates as future anti-adhesion drugs for bacterial diseases. *Glycoconjugate Journal*, 17, 659–664.
- Silva, S. S., Goodfellow, B. J., Benesch, J., Rocha, J., Mano, J. F., & Reis, R. L. (2007). Morphology and miscibility of chitosan/soy protein blended membranes. *Carbohydrate Polymers*, 70, 25–31.
- Simoni, S. F., Bosma, T. N. P., Harms, H., & Zehnder, A. J. B. (2000). Bivalent cations increase both the subpopulation of adhering bacteria and their adhesion efficiency in sand columns. *Environmental Science and Technology*, 34, 1011–1017.
- Sing, K. S. W., Everett, D. H., Haul, R. A. W., Moscou, L., Pierotti, R. A., Rouquerol, J., et al. (1985). Reporting physisorption data for gas/solid systems. *Pure and Applied Chemistry*, 57, 603–619.
- Sipahigil, O., & Dortunc, B. (2001). Preparation and in vitro evaluation of verapamil HCl and ibuprofen containing carrageenan beads. *International Journal of Pharmaceutics*, 228, 119–128.
- Sletmoen, M., Maurstad, G., Sikorski, P., Smestad Paulsen, B., & Stokke, B. T. (2003). Characterisation of bacterial polysaccharides: Steps towards single molecular studies. *Carbohydrate Research*, 338, 2459–2475.
- Stephen, S. M., Phillips, G. O., & Williams, P. A. (Eds.). (2006). *Food polysaccharides and their applications*. Boca Raton: Taylor & Francis.
- Sugita-Konishi, Y., Sakanaka, S., Sasaki, K., Juneja, L. R., Noda, T., & Amano, F. (2002). Inhibition of bacterial adhesion and salmonella infection in BALB/c mice by sialyloligosaccharides and their derivatives from chicken egg yolk. *Journal of agricultural and food chemistry*, 50, 3607–3613.
- Tirrell, M., Kokkoli, E., & Biesalski, M. (2002). The role of surface science in bioengineered materials. *Surface Science*, 500, 61–83.
- Trens, P., Denoyel, R., & Glez, J. C. (2004). Comparative adsorption of argon and nitrogen for the characterisation of hydrophobized surfaces. *Colloids and Surfaces A-Physicochemical and Engineering Aspects*, 245, 93–98.
- Tsvintzels, I., Pavlidou, E., & Panayotou, C. (2007). Biodegradable polymer foams prepared with supercritical CO_2 -ethanol mixtures as blowing agents. *Journal of Supercritical Fluids*, 42, 265–272.
- Tufenkji, N., Dixon, D. R., Considine, R., & Drummond, C. J. (2006). Multi-scale cryptosporidium/sand interactions in water treatment. *Water Research*, 40, 3315–3331.
- Vachoud, L., Zydowicz, N., & Domard, A. (1997). Formation and characterisation of a physical chitin gel. *Carbohydrate Research*, 302, 169–177.
- Valentin, R., Bonelli, B., Garrone, E., Di Renzo, F., & Quignard, F. (2007). Accessibility of the functional groups of chitosan aerogel probed by FT-IR-monitored deuteration. *Biomacromolecules*, 8, 3646–3650.
- Valentin, R., Horga, R., Bonelli, B., Garrone, E., Di Renzo, F., & Quignard, F. (2006). FTIR spectroscopy of NH_3 on acidic and ionotropic alginate aerogels. *Biomacromolecules*, 7, 877–882.
- Valentin, R., Molvinger, K., Quignard, F., & Di Renzo, F. (2005). Methods to analyse the texture of alginate aerogel microspheres. *Macromolecular Symposia*, 222, 93–101.
- Valentin, R., Molvinger, K., Viton, C., Domard, A., & Quignard, F. (2005). From hydrocolloids to high specific surface area porous supports for catalysis. *Biomacromolecules*, 6, 2785–2792.
- van Loosdrecht, M. C. M., Lyklema, J., Norde, W., & Zehnder, A. (1989). Bacterial adhesion—A physicochemical approach. *Microbial Ecology*, 17, 1–15.
- Vincent, T., & Guibal, E. (2004). Chitosan-supported palladium catalyst. 5. Nitrophenol degradation using palladium supported on hollow chitosan fibers. *Environmental Science and Technology*, 38, 4233–4240.
- Walter, R. H. (1998). *Polysaccharide dispersions*. San Diego: Academic Press.
- Wang, H., Fang, Y. E., & Yan, Y. (2001). Surface modification of chitosan membranes by alkane vapor plasma. *Journal of Materials Chemistry*, 11, 1374–1377.
- White, R. J., Budarin, V. L., & Clark, J. H. (2008). Tuneable mesoporous materials from α -D-polysaccharides. *ChemSusChem*, 1, 408–411.
- Yasuda, T., & Okuno, T. (1994). Contact angle of water on polymer surfaces. *Langmuir*, 10, 2435–2439.